Guanine Specific Binding at a DNA Junction Formed by d[CG(5-BrU)ACG]$_2$ with a Topoisomerase Poison in the Presence of Co^{2+} Ions[†,‡]

James H. Thorpe,[§] Jeanette R. Hobbs,[§] Alan K. Todd,[§,||] William A. Denny,[⊥] Peter Charlton,[#] and Christine J. Cardin*[,§]

Department of Chemistry, The University of Reading, Whiteknights, Reading RG6 6AD, U.K., Auckland Cancer Society Research Centre, Faculty of Medical and Health Sciences, The University of Auckland, Private Bag 92109, Auckland, New Zealand, and Xenova plc, 240 Bath Road, Slough, U.K.

Received July 26, 2000; Revised Manuscript Received September 18, 2000

ABSTRACT: The structure of the duplex d[CG(5-BrU)ACG]$_2$ bound to 9-bromophenazine-4-carboxamide has been solved through MAD phasing at 2.0 Å resolution. It shows an unexpected and previously unreported intercalation cavity stabilized by the drug and novel binding modes of Co^{2+} ions at certain guanine N7 sites. For the intercalation cavity the terminal cytosine is rotated to pair with the guanine of a symmetry-related duplex to create a pseudo-Holliday junction geometry, with two such cavities linked through the minor groove interactions of the N2/N3 guanine sites at an angle of 40°, creating a quadruplex-like structure. The mode of binding of the drug is shown to be disordered, with the major conformations showing the side chain bound to the N7 position of adjacent guanines. The other end of the duplex exhibits a terminal base fraying in the presence of Co^{2+} ions linking symmetry-related guanines, causing the helices to intertwine through the minor groove. The stabilization of the structure by the intercalating drug shows that this class of compound may bind to DNA junctions as well as duplex DNA or to strand-nicked DNA ('hemi-intercalated'), as in the cleavable complex. This suggests a structural basis for the dual poisoning of topoisomerase I and II enzymes by this family of drugs.

Topoisomerases are responsible for the interconversion of the topological states of DNA. These enzymes generate transient single or double strand breaks in the DNA phosphodiester backbone to allow the passage of one (topo I) or two (topo II) DNA strands during replication, resulting in an associated relaxation of their supercoiled state. Some DNA-intercalating compounds, including tricyclic carboxamides (Figure 1a) have the unusual ability to poison topoisomerases of both types I and II, which is striking due to the structural diversity of these enzymes. Topo I activity is associated with two protein folds and two proposed mechanisms known as the strand passage (IA) and controlled rotation (IB) mechanisms (*1*, *2*). The controlled rotation mechanism is that proposed for type IB topos (the human enzyme) for which structures are available for the initial protein−DNA complex (*3*), and also for the cleaved complex, in which the enzyme is covalently bound, through a 3′-phosphotyrosine linkage, to a 22-mer DNA duplex at the nick site. There is also a structural homology between a family of site-specific recombinases (*4*, *5*) (also known as tyrosine recombinases) and this class of topo, and it has been proposed that the fundamental difference between these activities lies in the degree of association of the protein (topoisomerase activity is possible for the monomeric protein, but recombinase activity would require association). It is not clear whether assays for topo I poisoning have included assays for inhibition of recombination, but their two activities may be related. Vaccinia virus topo I has a structure very similar to that of the human enzymes and also has been shown to catalyze the resolution of the four-way DNA Holliday junctions (*6*), which are key intermediates in general homologous recombination processes.

Topo II is targeted to supercoiled DNA, which it may recognize through cruciforms, helix−helix crossovers, and hairpins (*7*). It has a higher affinity for Z-DNA than B-DNA, can cleave DNA hairpins, and has recently been shown to bind to and cleave a DNA four-way junction in vitro, by binding to the center of the junction, having a 4-fold higher affinity for the junction than for the duplex (*8*).

We have previously shown (*9*, *10*) that related 9-aminoacridinecarboxamides (e.g., **3**)—which are selective topo II poisons—can intercalate into duplex DNA, with the carboxamide side chain orientated by H-bonding to the cationic ring nitrogen of the acridine to lie in the major groove and specifically bind to one of these adjacent guanines (N7/O6). This work (*11*) has revealed at near-atomic resolution (*9*, *12*) the importance of disorder within the intercalation cavity and of the state of protonation of the drug on the binding modes, together with the backbone disorder induced by the

[†] This work was supported by an EPSRC Studentship (to J.R.H.), a University of Reading Studentship (to J.H.T.), and Xenova plc.

[‡] NDB reference DD0026; PDB reference 1eg6.

* Corresponding author. E-mail: c.j.cardin@reading.ac.uk. Phone: 44-118-9318215. Fax: 44-118-9316632.

[§] University of Reading.

[||] Present address: CRC Biomolecular Structure Unit, Chester Beatty Laboratories, Institute of Cancer Research, 237 Fulham Road, London SW3 6JB, U.K.

[⊥] University of Auckland.

[#] Xenova plc.

10.1021/bi001749p CCC: $19.00
Published on Web 11/10/2000

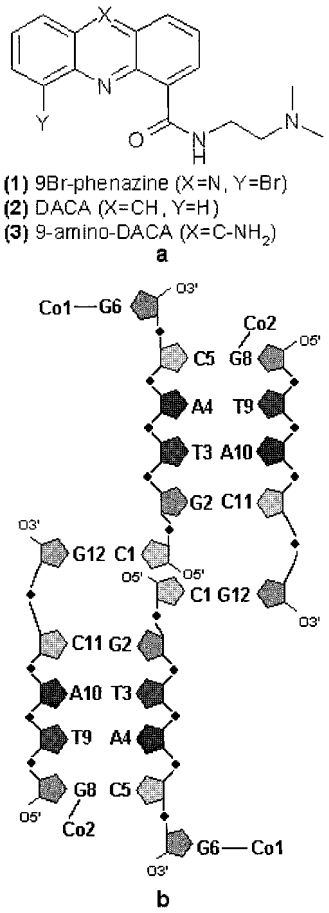

FIGURE 1: (a) Structural formulas of the tricyclic drug systems. (b) Labeling scheme for the oligonucleotide and bound cobalt ions. The junction-like formation is shown (C1 with G12 from a symmetry-related hexamer). Quadruplex formation between G2/C11 and C1/G12 is not shown (see Figures 2b,c and 4a).

drug and by replacement of thymine by 5-bromouridine (introduced as an anomalous scatterer). It showed that N7 of guanine was the single most important binding site for the flexible drug side chain. Three closely related structures were refined *(12*, *13*) without revealing any cationic binding sites other than the drug but providing the first structural characterization of a specific major groove interaction in a synthetic monointercalator. Three drug molecules per symmetric duplex were bound, the third acting as a spacer between the duplexes in a quasi-infinite stack.

A particularly interesting subclass of these compounds are the deamino analogues, represented by **2** (XR5000/DACA), a drug currently in clinical trials (*14*). This is a dual poison of both topo I and II (*15*), which is of therapeutic value in avoiding resistance due to topo isozyme switching (*16*). The structure of a bromo analogue (**1**) of a dual poison (phenazine-1-carboxamide) (*17*) with the DNA duplex d(CGTACG)$_2$ was undertaken to see whether these compounds, with a quite different biological profile compared to **3**, bound differently to DNA. Our crystallographic study was intended to highlight the structural features expected to be important in determining this behavior, with the underlying assumption being that more than one binding orientation would be a prerequisite for mixed poisoning, as suggested for intoplicine analogues (*18*). Most of the known dual poisons combine high affinity for DNA intercalation with flexible side chains capable of more than one DNA groove or protein interaction. While the side chain of the tricyclic carboxamide family appears to bind specifically to CG/CG base pairs, the intercalated carboxamide may have multiple orientations, relating to the possible side chain hydrogen bond patterns, as intercalation renders the two guanine binding sites inequivalent stereochemically.

We now report the structure of **1** (9-bromophenazine-1-carboxamide) bound to the same DNA sequence. This structure is surprisingly novel.[1] Although the data consistently showed a 9-fold stacking repeat apparently similar to that seen in the previous work, it is generated in a totally different manner, with the repeating unit now comprising two duplexes and a drug, with an unexpected DNA quadruplex at the intercalation cavity. Co^{2+}-induced fraying at the other end of the duplex reduced the six base pairs of each duplex to four. More surprisingly, this quadruplex-like cavity also shows Holliday junction-like features. The intercalation cavity is generated both by N2−N3 guanine−guanine H-bonding, giving the quadruplex, and by terminal cytosine strand exchange. The most closely similar published structure is that of a copper(II) tetrapyridylporphyrin complex with the sequence d(CGATCG)$_2$ (*19*), which, although it has a positively charged periphery, is much larger and could not be accommodated within a normal intercalation cavity.

MATERIALS AND METHODS

The self-complementary DNA hexamer d[CG(5-BrU)ACG] was purchased from Oswel DNA service (University of Southampton, U.K.). Crystals were grown by vapor diffusion at 291 K from sitting drops containing 1 μL of 0.5 mM DNA (double-stranded concentration), 2 μL of 0.5 mM drug, 2 μL of 40 mM sodium cacodylate buffer, pH 6.0, 1 μL of 40 mM Mg(OAc)$_2$, 2 μL of 12 mM $CoCl_2$, and 2 μL of 30% 2-methyl-2,4-pentanediol, equilibrated against a 1 mL reservoir of 35% 2-methyl-2,4-pentanediol. Clear diamond-shaped crystals grew over a period of about 15 months.

Data collection was carried out at 100 K on a crystal of dimensions approximately 0.25 × 0.25 × 0.3 mm^3 on beamline X31 at the DESY synchrotron facility (Hamburg, Germany) using a Mar 345 image plate detector in dose and small Mar mode. Wavelengths were recorded initially from a fluorescence spectrum measured from a powdered sample of bromouridine (*20*) and later from the crystal to maximize the anomalous and dispersive signals resulting in the measurement of five wavelengths (Table 1). Data processing was carried out using MOSFLM (*21*) and SCALA (*22*), yielding the final cell parameters $a = 29.42$ Å, $b = 53.44$ Å, and $c = 41.32$ Å for the orthorhombic space group *C*222, with two heavy atom positions determined by SOLVE (*23*) and phase calculations carried out with MLPHARE and DM (*22*) used for solvent flattening. The initial model was built ab initio into the 2 Å MAD map with the map fitting program XFIT from the XTALVIEW suite (*24*). The nucleic acid backbone and bases could all be traced in the MLPHARE/DM phased map, whereas the drug density was not clearly revealed until the end of the refinement due to its disorder. The cobalt ions were identified by their peak heights and their molecular geometries, and their coordination environ-

[1] Note added in proof: While this paper was being processed, an independent report of a very similar nucleic acid structure was published (*39*).

Table 1: Data Collection, Phasing, and Refinement Statistics

	inflection point		whiteline max		
	BrU[a]	xtal[b]	(BrU)[a]	remote 1	remote 2
λ (Å)	0.9208	0.9201	0.9192	0.9000	1.1000
resolution range (Å)	26.6−2.0	26.6−2.0	26.6−2.0	26.6−2.0	25.9−2.25
unique reflections	2215	2211	2218	2372	1454
completeness (%)[c]	98.7 (91.0)	98.9 (92.5)	98.9 (92.5)	99.5 (93.3)	89.7 (93.6)
multiplicity	3.4	3.4	3.4	3.4	2.4
R-merge[c,d]	8.0 (30.8)	8.0 (30.8)	7.6 (32.5)	8.9 (36.3)	7.1 (25.6)
R-merge (anom)[c,e]	7.2 (30.1)	7.2 (30.1)	6.9 (31.4)	7.3 (34.1)	6.9 (20.0)
anom data comp (%)[c,f]	98.0 (87.8)	98.0 (87.4)	98.3 (89.0)	98.7 (94.3)	73.9 (78.3)
R-Cullis[g] (acentric/centric)		0.95/0.96	0.98/1.01	0.80/0.62	0.77/0.60
phasing power[h] (acentric/centric)		0.48/0.46	0.28/0.28	1.32/1.50	1.60/1.71
reflections (acentric/centric)	1748/451	1750/453	1755/457	1749/448	1171/269
DNA atoms				229	
water molecules				33	
R-factor[i]				18.58	
R-free[j]				27.62	

[a] Fluorescence spectrum measured from the powdered Br-U sample. [b] Fluorescence spectrum measured from the cryo-cooled crystal sample. [c] Values in parentheses correspond to the outermost resolution shell. [d] $R\text{-merge} = \sum_{hkl}\sum_i|I_1(hkl) - \langle I(hkl)\rangle|/\sum_{hkl}\sum_i I_1(hkl)$, calculated for the whole data set. [e] $R\text{-merge (anomalous)} = \sum_{hkl}\sum_i|I_1(hkl\pm) - \langle I(hkl)\rangle|/\sum_{hkl}\sum_i I_1(hkl\pm)$. [f] Percentage of reflections with a Bijvoet pair. [g] *R*-Cullis is the mean residual lack of closure error divided by the dispersive difference. [h] Phasing power = rms ($|F_H|/E$), where F_H is the heavy atom amplitude and E is the residual lack of closure error. [i] $R\text{-factor} = \sum_{hkl}||F_o(hkl)| - k|F_c(hkl)||/\sum_{hkl}|F_o(hkl)|$. [j] *R*-factor for 10% of the reflections not used in the refinement.

ments were modeled as octahedral aquated ions. Crystallographic refinement was carried out using the program SHELX97 (*25*) with SHELXPRO used to produce sigma-A and difference maps for final model building and SHELXWAT to carry out the initial water divining procedures. Isotropic temperature factors were used for all atoms except Br and Co, which were given individual anisotropic temperature factors. The 0.9000 Å data set was used for refinement, with refinement statistics shown in Table 1. Neutral atom scattering factors were used for all atoms except Co, which were treated as Co^{2+} ions. Dictionary values were used for the nucleic acid bond lengths and angles with no torsional restraints (*26*, *27*). The final model includes 11 nucleic acid residues (the base and sugar of cytosine 7 were omitted as there was no visible density for either), 1 disordered drug molecule (50% occupancies of sites assumed), 1.5 Co^{2+} ions, and 31 waters. The coordinates and structure factors have been deposited with the NDB (DD0026). Table 2 (Supporting Information) shows the backbone torsion angles and Table 3 (Supporting Information) the derived morphology parameters, the latter adhering as closely as possible to current NDB conventions (*28*) and calculated using Curves 5.1 (*29*). Figure 1a shows the drug structure and Figure 1b the nucleic acid numbering. All references to the C1/G12 base pair are to the symmetry equivalent C1 (at $-x, y, -z$).

RESULTS

Crystals of the duplex d[CG(5-BrU)ACG]$_2$ with 9-bromophenazine-4-carboxamide (**1** in Figure 1a) in the orthorhombic space group *C*222 were only obtained in the presence of Co^{2+} ions. The asymmetric unit (Figure 2a) contains one duplex, with an overall B-DNA central four base pairs and a deformation at either end of the helix, 1 disordered drug, and 1.5 cobalt ions per asymmetric unit—1 cobalt ion (Co1) lies on a special position on a dyad axis. Figure 3 shows the quality of the MLPHARE-DM phased MAD map and also the two cobalt environments. The two strands of the duplex, though chemically identical, behave in a quite distinct fashion, in contrast to the symmetrical behavior found with the 9-aminoacridines complexed to the same nucleic acid sequence. Normal base pairing is found only for the central four base pairs, with two diverse modes of fraying observed at the two ends. There is no direct relationship between the symmetry of the self-complementary DNA duplex and the crystallographic symmetry elements, unlike the 9-aminoacridine structures which have a crystallographic 2-fold axis running through the center of the symmetrically intercalated duplex (*9*). In this case, because of the fraying of the terminal base pairs, the two symmetry-related C5/G8 base pairs are actually stacked onto each other, bringing the cobalt ions bound to G8 (Co2) to within 7.5 Å of each other and linked by water molecules. The N7 positions of two symmetry-related G6 residues at the cobalt frayed end are linked by a second cobalt ion (Co1) generating a *trans* coordination geometry at the cobalt ion (Figure 3c). The G6 residue is folded back from the helix axis to lie in the minor groove of the duplex, and the grooves of the symmetry-related duplexes are interlocked. The unpaired cytosine thus generated is disordered in the crystal lattice protruding into the solvent space of the major groove. It can form no obvious interactions, and no clear model could be built for this residue [both of these phenomena have been previously observed for Ni^{2+} ions bound to the sequence d(CGTATATACG)$_2$ with minor groove binding drug netropsin (*30*)]. The G2/C11 base pair exhibits a normal hydrogen-bonding pattern; however, the terminal base pair (C1/G12) is formed by the junction-like strand exchange of the terminal C1, shown schematically in Figure 1b, and superimposed on the final sigma-A map in Figure 4a. Two quasi-continuous stacks in the lattice are arranged in a Holliday junction-like fashion (*31*, *32*), with helix axes aligned at approximately 60°, the C1 crossover and Co1 cross-linking creating a three-dimensional network. The solvent channels within this packing also run between these crossed-over helices. Only one drug molecule is bound per duplex (irrespective of the ratio used in crystallization), between the C1/G12 and G2/C11 base pairs. The C1/G12 base pair hydrogen bond lengths show compression toward the minor groove side, in contrast to the unstrained values

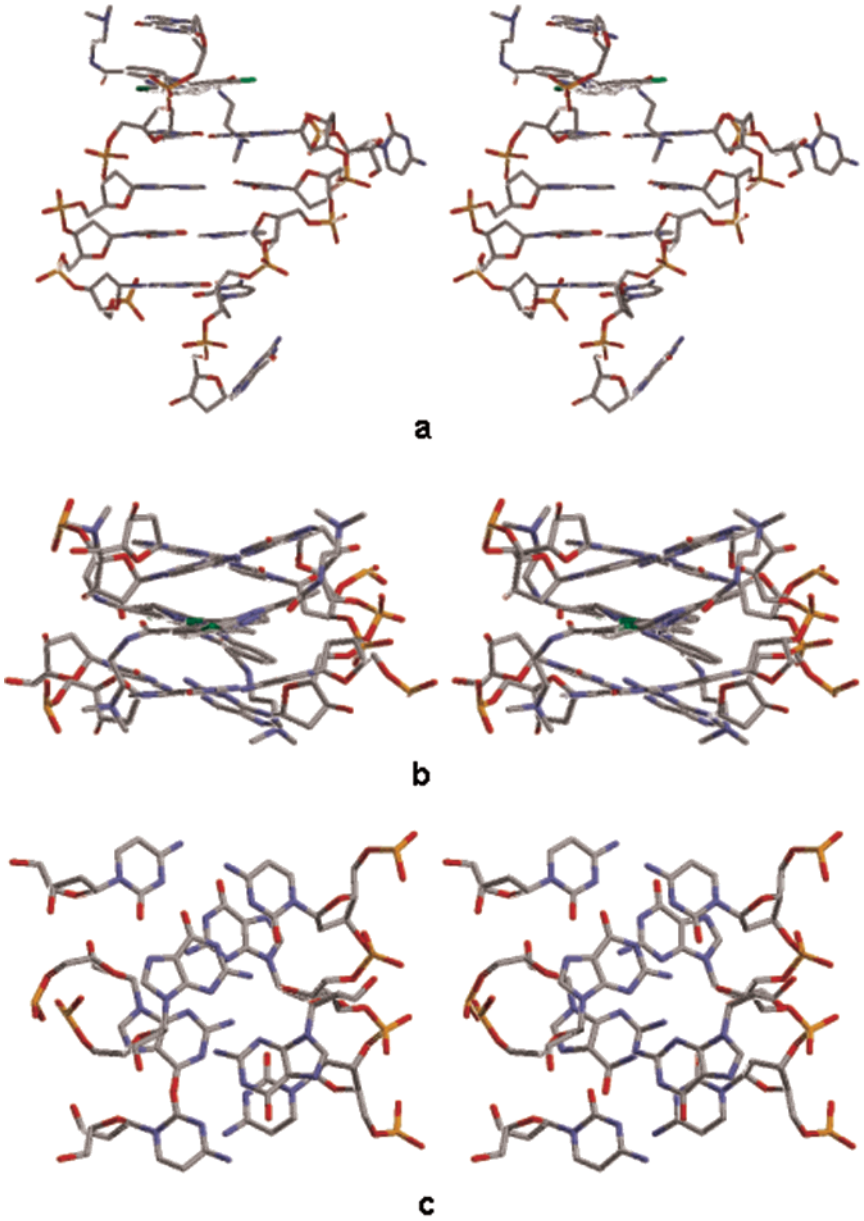

FIGURE 2: (a) Stereoview into the minor groove showing the unusual conformation of the hexamer d[CG(5-BrU)ACG]$_2$. Water molecules and metal ions are omitted for clarity. The two disordered drug conformations are shown overlapping. (b) Stereoview of the intercalation cavity showing both disordered drug orientations. The open junction side of the cavity is on the left. The cavity has 2-fold symmetry but for clarity is shown in an off-axis projection. (c) Stereoview of the cavity without drug molecules, with the open side of the cavity on the left. For clarity an off-axis projection has been used.

shown for the G2/C11 base pair, and in consequence, the calculation of base morphology parameters is more meaningful for the single-stranded values (see Table 3 in Supporting Information). Most characteristic is the high G12−C11 twist angle of 45°, with a C4′-*exo* sugar conformation (δ 99°) and a χ angle of −135° at the G2 of the junction (see Table 2 in Supporting Information). Taking our previous work to be a "normal" intercalation mode for these compounds, the twist angle at an intercalation site (CG/CG) is expected to be 25°, 28° at the adjacent step (GT/AC in our work), rising to 46° at the central TA/TA step in d(CGTACG)$_2$. The present structure almost reverses this pattern (see Table 3 in Supporting Information).

The base pairs of this unusual cavity are further linked by G2/G12 N2−N3 hydrogen bonds in the minor groove across the floor (and roof by symmetry) of the intercalation cavity (Figures 2 and 4a), so that the overall architecture is two such linked cavities. The two guanine bases of this quadruplex are inclined at an angle of 40° to each other, generating a bend in the overall helix axis of the quasi-continuous stacking.

The unusual intercalation cavity at the junction of the helices has facilitated a mixed mode of binding for the 9-bromophenazine chromophore. Its location could only be determined from an omit map calculated toward the end of the refinement (Figure 4b). Repeated SOLVE runs did not yield the disordered drug Br positions from the MAD data, but this fits our previous experience (*9*). In both cases only one chemically distinct kind of Br was actually located from its anomalous and dispersive behavior (in the previous work it was the Br on the uridine which was hard to locate, even from 1.2 Å MAD data), and we conclude that the difficulty

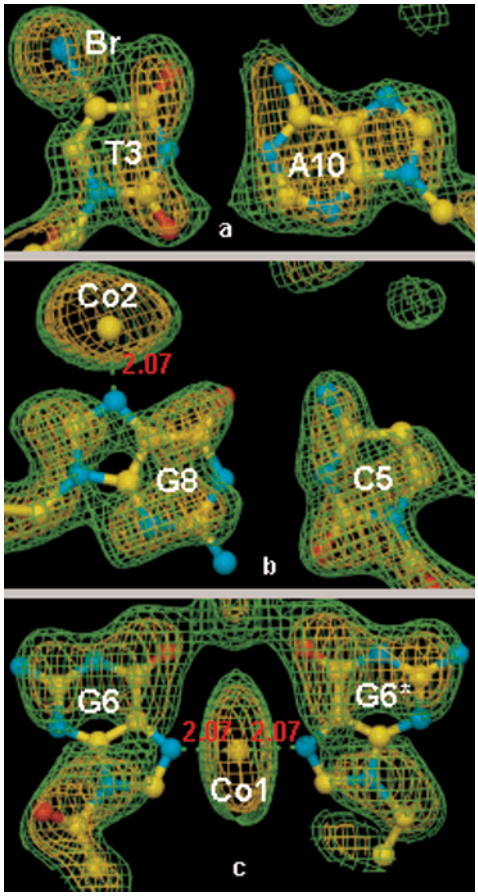

FIGURE 3: Three views of the 2 Å MAD electron density map used to build the initial model: (a) the T3 (5-BrU)/A10 base pair showing bromine density, (b) Co2 bound to the guanine N7 of G8, and (c) Co1 on a special position with *trans* coordination to symmetry-related N7 on G6. The phases were calculated by MLPHARE with solvent flattening carried out by DM. Green = 1σ and yellow = 2σ.

may reflect the precise inflection point wavelength used. The drug was fitted with two distinct orientations shown, with $-NMe_2H^+$ of the side chain H-bonded to each of the guanine N7 sites in the major groove (Figure 5). With the drug "hemi-intercalated" into each strand in either orientation, the cavity thus has an "open" and a "closed" side, unlike a normal intercalation cavity as found in our previous work. In further contrast to our previous results, the neutral N10 in the chromophore of the phenazine has not generated any direct hydrogen bonds to the carboxamide side chain of the drug. The observation of two such hydrogen-bonding modes in a single crystal was a telling feature of our previous study (*9*). It highlighted the importance of pK_a and charge neutralization in controlling side chain orientation in the 9-aminoacridine series. Here, the neutral chromophore does not H-bond to the carboxamide NH. Instead, side chain orientation is determined by the location of the N7/O6 lone pairs of the guanines in the major groove. This greater orientational flexibility would be consistent with dual topo poisoning. In one orientation of the disordered drug (shown in blue in Figure 5), long axes of drug and base pairs are approximately aligned, and the carboxamide plane [C(phenazine)−(C═O)−NH−) is rotated by 13° with respect to the phenazine plane. This component of the disorder forms the hydrogen bond to the "hemi-intercalating" G12, length 2.71 Å. Conversely, the second orientation (shown in red) has a threading orientation with respect to the G2/C11 base pair and also has some stacking interaction with C1, and the carboxamide plane makes an angle of 20° to the phenazine plane. This $-NMe_2H^+$ group is hydrogen bonded to N7 of guanine G2, the junction-forming residue, length 2.69 Å. In this position the positive charge of $-NMe_2H^+$ is equidistant from O1P (4.62 Å) and O2P (4.76 Å) of G2 (the phosphate oxygens of the junction). No metal cation can be located near to the phosphates, and as close approach of phosphate groups requires some neutralization of their electrostatic potential, it seems likely that this dimethylammonium group is playing this role, anchored by the stacking force of intercalation.

DISCUSSION

X-stacked junction formation requires cations, and in this structure the cationic side chain seems to play a role in stabilizing the novel DNA conformation. Junctions have been known for some time to provide a high-affinity binding site for intercalators (*33*), and they may stabilize the X-stacked form by charge neutralization as does Mg^{2+} (*34*). Resolution of these junctions can occur by resolvase enzymes but also some eukaryotic topo I enzymes (*6*, *35*). Human topo IIβ has also recently been shown to preferentially bind to such sites (*8*). Our observations may therefore have pharmacological relevance to the preferred mode of binding of these compounds to DNA junctions and the formation of the topoisomerase ternary complex, but this will have to be confirmed by further work. We could only obtain crystals between these compounds and this oligonucleotide in the presence of Co^{2+} ions, so, in principle, we cannot be sure that the structure we observe is not partly due to the presence of this metal ion. The role of Co1 in linking the symmetry-related G6 residues is clear, but while this is important in generating the crystal form, the same mode of linking, by Ni^{2+} ions, has been found in the crystal lattice of a DNA−netropsin complex (*30*), and so does not necessarily have any bearing on the formation of the novel intercalation cavity. We also note that the nearer Co^{2+} site (Co2) is more than 11 Å distant from the junction phosphate oxygen G2 O2, making a direct electrostatic effect of this Co^{2+} on the junction stabilization unlikely, given that the $-NMe_2H^+$ side chain is about 4.5 Å from the same atom. We therefore believe that the primary stabilizing interaction of this unusual DNA cavity is that created by the drug side chain.

The tricyclic carboxamides differ from the camptothecins (topo I poisons) in binding to duplex DNA, and their poisoning mechanism may well involve a different binding mode from that proposed for camptothecin (*36*, *37*). The number of specific interactions formed by this class of compounds is clearly less than for camptothecin, with only the carboxamide side chain capable of forming specific hydrogen bonds. Modeling studies of camptothecin bound to this site proposed specific drug−DNA and drug−protein interactions based on plausible conformational changes in the cleaved DNA strand on the 5′ side of the putative drug binding site (*36*). In this model the base adjacent to the cleavage site is rotated to stack onto the drug chromophore, separating the free 5′-OH from the phosphotyrosine residue by 4.5 Å. An alternative model is intercalative, with an alternative orientation of the camptothecin chromophore (*37*). Neither model can account completely for all of the observed structure−activity relationships. Our present structure sug-

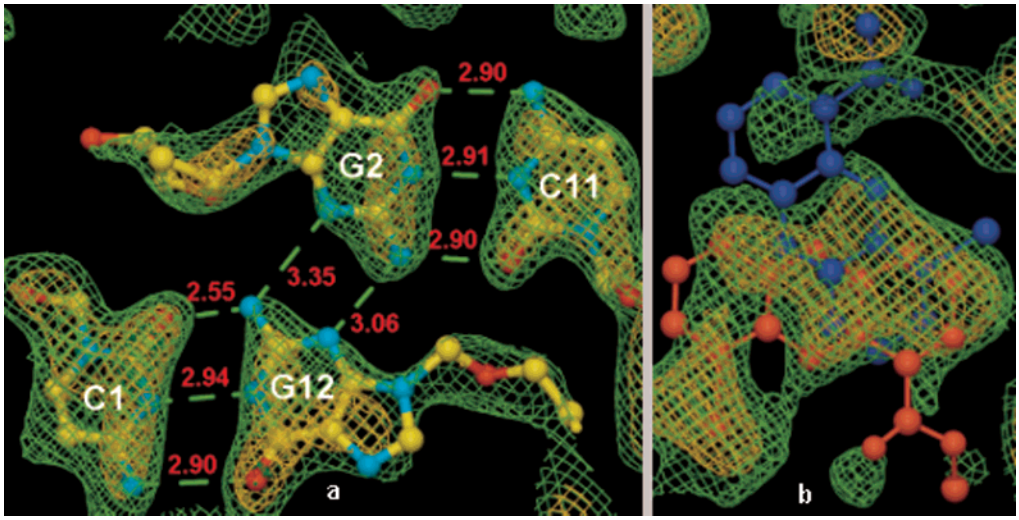

FIGURE 4: (a) A 2 Å sigma-A map illustrating the floor (and roof by symmetry) of the intercalation cavity, showing the hydrogen-bonding pattern of the bases and the minor groove interactions of G2, G12 through N2, and N3. Green = 1σ and yellow = 2σ. (b) Calculated omit map at a resolution of 2 Å for the disordered drug system with the intercalation cavity. Green = 0.5σ and yellow = 1σ.

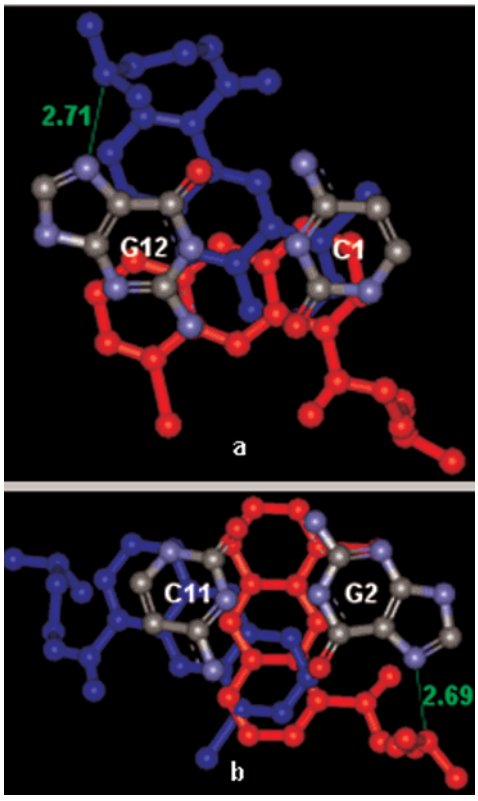

FIGURE 5: Two views of the disordered drug system and its stacking interaction with the two adjacent C/G base pairings of the intercalation cavity. Side-chain hydrogen bonds to guanine N7 sites on G12 (first orientation in blue) and G2 (second orientation in red) are also shown. Note the threading orientation of the second component with respect to the G2/C11 base pair only.

gests a plausible model for the interaction of the tricyclic carboxamide class of compounds with topoisomerases, which may be relevant to their unusual dual topoisomerase poisoning ability and their functionally distinct mode of action (*38*). The hemi-intercalative binding seen here suggests a structure where the phosphotyrosine linkage in the trapped cleavable complex would take the place of the Holliday junction-like feature seen in the above complex. Further work is in progress to extend our observations.

ACKNOWLEDGMENT

We acknowledge access to the EMBL Hamburg synchrotron facility at DESY, supported by the TMR/LSF (contract no. ERBFMGECT980134) and HPRI (contract no. HPRI-CT-1999-00017) programs of the European Union. We thank Professor S. Neidle and Drs. H. R. Powell, E. Garman, and P. R. Evans for helpful discussions.

SUPPORTING INFORMATION AVAILABLE

Two tables giving backbone torsion angles and base morphology parameters. This material is available free of charge via the Internet at http://pubs.acs.org.

REFERENCES

1. Redinbo, M. R., Champoux, J. J., and Hol, W. G. J. (1999) *Curr. Opin. Struct. Biol. 9*, 29−36.
2. Wigley, D. B. (1998) *Structure 6*, 543−548.
3. Redinbo, M. R., Stewart, L., Kuhn, P., Champoux, J. J., and Hol, W. G. J. (1998) *Science 279*, 1504−1513.
4. Guo, F., Gopaul, D. N., and Van Duyne, G. D. (1997) *Nature 389*, 40−46.
5. Lee, J., Tribble, G., and Jayaram, M. (1999) *J. Mol. Biol. 296*, 403−419.
6. Sekiguchi, J., Cheng, C., and Shuman, S. (2000) *Nucleic Acids Res. 28*, 2658−2663.
7. Berger, J. M. G., Gamblin, S. J., Harrison, S. C., and Wang, J. C. (1998) *Nature 379*, 225−232.
8. West, K. L., and Austin, C. A. (1999) *Nucleic Acids Res. 27*, 984−992.
9. Todd, A. K., Adams, A., Thorpe, J. H., Denny, W. A., Wakelin, L. P. G., and Cardin, C. J. (1999) *J. Med. Chem. 42*, 536−540.
10. Adams, A., Guss, M., Collyer, C., Denny, W. A., and Wakelin, L. P. G. (1999) *Biochemistry 38*, 9221−9023.
11. Todd, A. K. (1999) Ph.D. Thesis, University of Reading.
12. Todd, A. K., Thorpe, J. H., Adams, A., Powell, H. R., Hinds, E., Denny, W. A., Wakelin, L. P. G., and Cardin, C. J. (2000) unpublished experiments.
13. Thorpe, J. H. (2000) Ph.D. Thesis, University of Reading.
14. De Bono, J. S., Propper, D., Ellard, S., Steiner, J., Bevan, P., Doobs, N., Flanagan, E., Ganesan, T. S., Talbot, D. C., Campbell, S., Twelves, C., and Harris, A. (1998) *Ann. Oncol. 9*, 117.
15. Atwell, G. J., Rewcastle, G. M., Baguley, B. C., and Denny, W. A. (1987) *J. Med. Chem. 30*, 664−669.

16. Stewart, A. J., Dangerfield, W., Lancashire, H., Mistry, P., Okiji, S., Baguley, B., Denny, W. A., Templeton, D., and Charlton, P. (1999) *Clin. Cancer Res. 5*, 3864s.
17. Rewcastle, G. W., Denny, W. A., and Baguley, B. C. (1987) *J. Med. Chem. 30*, 843−851.
18. Nabiev, I., Chourpa, I., Riou, J.-F., Nguyen, Ch., Lavelle, F., and Manfait, M. (1994) *Biochemistry 33*, 9013−9023.
19. Lipscomb, L. A., Zhou, F. X., Presnell, S. R., Woo, R. J., Peek, M. E., Plaskon, R. R., and Williams, L. D. (1996) *Biochemistry 35*, 2818−2823.
20. Todd, A. K., Adams, A., Powell, H. R., Wilcock, D. J., Thorpe, J. H., Lausi, A., Zanini, F., Wakelin, L. P. G., and Cardin, C. J. (1999) *Acta Crystallogr., Sect. D: Biol. Crystallogr. 55*, 729−735.
21. Leslie, A. G. W. (1990) in *Crystallographic Computing*, Oxford University Press, Oxford, U.K.
22. CCP4 Project (1994) *Acta Crystallogr., Sect. D: Biol. Crystallogr. 50*, 760−793.
23. Terwilliger, T. C., and Berendzen., J. (1999) *Acta Crystallogr., Sect. D: Biol. Crystallogr. 55*, 849−861.
24. McRee, D. E. (1992) *J. Mol. Graphics 10*, 44−46.
25. Sheldrick, G. M., and Schneider, T. R. (1997) *Methods Enzymol. 277*, 319−343.
26. Gelbin, A., Schneider, B., Clowney, L., Hsieh, S., Olson, W. K., and Berman, H. M. (1996) *J. Am. Chem. Soc. 118*, 519−529.
27. Clowney, L., Jain, S. C., Srinivasan, S. R., Westbrook, J., Olson, W. K., and Berman, H. M. (1996) *J. Am. Chem. Soc. 118*, 509−518.
28. Nucleic Acid Databank, http://ndbserver.rutgers.edu.
29. Lavery, R., and Sklenar, H. (1998) *Biomol. Struct. Dyn. 6*, 63−91.
30. Abrescia, N. G. A., Malinina, L., and Subirana, J. A. (1999) *J. Mol. Biol. 294*, 657−666.
31. Eichman, B. F., Vargason, J. M., Mooers, B. H. M., and Ho, P. S. (2000) *Proc. Natl. Acad. Sci. U.S.A. 97*, 3971−3976.
32. Ortiz-Lombardia, M., Gonzalez, A., Eritja, R., Aymami, J., Azorin, F., and Coll, M. (1999) *Nat. Struct. Biol. 6*, 913−917.
33. Guo, Q., Lu, M., Seeman, N. C., and Kallenbach, N. R. (1990) *Biochemistry 29*, 1614−1624.
34. Duckett, D. R., Murchie, A. I. H., and Lilley, D. M. J. (1990) *EMBO J. 9*, 583−590.
35. Sekiguchi, J. A., Seeman, N. C., and Shuman, S. (1996) *Proc. Natl. Acad. Sci. U.S.A. 93*, 785−789.
36. Stewart, L., Redinbo, M. R., Qiu, X., Hol, W. J. G., and Champoux, J. J. A. (1998) *Science 279*, 1534−1541.
37. Fan, Y., Weinstein, J. N., Kohn, K. W., Shi, L. M., and Pommier, Y. (1998) *J. Med. Chem. 41*, 2216−2226.
38. Stewart, A. J., Dangerfield, W., Koffler, B., Baguley, B., Denny, W. A., and Charlton, P. (2000) *Proc. Am. Assoc. Cancer Res., 91st 41*, 212.
39. Yang, X., Robinson, H., Gao, Y.-G., and Wang, A. H.-J. (2000) *Biochemistry 39*, 10950−10957.

BI001749P